International Journal of Nanoelectronics and Materials
Volume 13 (Special Issue) May 2020 [461-472]

Diffusion Mechanism of Silver Particles in Polymer Binder for Die Attach Interconnect Technology

S. R. Esa[1,4], G. Omar[1,2]*, S. H. Sheikh Md Fadzullah[1], K. S Siow[3], B. Abdul Rahim[4] and B. Çoşut[5]

[1]*Faculty of Mechanical Engineering, Universiti Teknikal Malaysia Melaka, Hang Tuah Jaya, 76100 Durian Tunggal, Melaka, Malaysia.*
[2]*Advanced Manufacturing Centre (AMC), Faculty of Mechanical Engineering, Universiti Teknikal Malaysia Melaka, Hang Tuah Jaya, 76100 Durian Tunggal, Melaka, Malaysia.*
[3]*Institute of Microengineering and Nanoelectronics, Universiti Kebangsaan Malaysia, 43600 Bangi, Selangor, Malaysia.*
[4]*MIMOS Semiconductor (M) Sdn. Bhd., Technology Park Malaysia, Bukit Jalil, 57000, Kuala Lumpur, Malaysia.*
[5]*Department of Chemistry, Gebze Institute of Technology, 41400 Kocaeli, Turkey.*

ABSTRACT

Sintered Ag has gained strong interest as an important alternative material for interconnect technology in wide bandgap (WBG) semiconductor industries specifically for high thermal dissipations and high-speed applications. This material typically consists of metallic particles bounded by polymer binder expected to diffuse at the temperature much lower than its melting temperature. This paper studies the diffusion mechanism between Ag particles and its microstructural change over different heat treatment temperature that leads to the understanding on the formation of bonding particles into a predominantly solid Ag network as a conducting path for the interconnect systems. The surface diffusion initiated between Ag particles as they come into intimate contact through the formation of necking. Further atomic movement and diffusion between the particles neck resulting in volume expansion, necking growth as well as the transformation of the particle shape from spherical into an elongated structure. This results in the formation of a long chain of connecting particles, which transform the Ag particles into a solid Ag network.

Keywords: Diffusion, Grain Size, Mechanism, Microstructure, Sintered Ag.

1. INTRODUCTION

Wide bandgap (WBG) semiconductors such as silicon carbide (SiC) and gallium nitride (GaN) are unanimously recognized as outstanding materials that will revolutionize the future of high power semiconductor applications, replacing the conventional Si-based semiconductors owing to their excellent properties by having superior energy efficiencies, higher temperature operations, high frequency and fast switching speed [1,2]. The performance and reliability of WBG technology comprise of not only the packaging material and structure but also their bonding interconnect especially die attach material as an essential component that must able to withstand severe and harsh environments [3]. This is because die attach material plays an important role in the thermal management of intrinsic heat generation and ensuring effective heat dissipation of the devices.

Commonly used lead-free solder (SAC305, SAC405) die attach materials have the characteristics of high thermal performance but suffered from the high-temperature process up to 326°C for the solder to reflow. This will result in the potential of interface stress generation within the interconnect system due to the coefficient of thermal expansion (CTE) mismatch between different material properties. Besides, the material has other metallurgical-joint issues that the

*Corresponding Author: *ghazali@utem.edu.my*

uncontrollable intermetallic growth lead to reliability degradation. Solder materials will also be greatly deteriorated at a higher temperature due to the low melting temperature. The metallic filled epoxy polymer-based die attach material allows low-temperature process but has poor performance in handling the high thermal dissipation. This is due to the polymer material, although filled with metallic filler, has poor thermal conductivity as a result of metal to polymer interface resistivity does not allow thermal to dissipate effectively. In summary, currently used die attach materials are impeded due to their inherent drawbacks, limited working temperature range, low heat dissipation, low melting temperature, poor thermal conductivity, susceptible to thermal fatigue-creep failure, crack and delamination at the interface due to intermetallic compound (IMC) growth and many other reliability issues [4-7].

On the other hand, sintered Ag interconnect technology is one of the promising alternatives to the inferior traditional die attach material as it perfectly addresses the needs in today's interconnect materials and has received much attention for the next generation of high-power electronics applications [8]. The importance of this research field is also reflected by a significant increase in the research paper and patent related to Sintered Ag as a workable technology [9, 10]. Sintered Ag allows sintering to be executed at relatively low temperature and yet it can be used in high-temperature environments exceeding 250°C, since the melting point of Ag is 961.8°C, it also exhibits excellent electrical and thermal conductivities [11,12]. Sintered Ag has demonstrated ability as an interconnect material in the appropriate conditions. Several factors affect the performance of sintered Ag, for instance, the pressure, temperature, time, Ag particle size distributions, a type of organic materials in the Ag paste, surface metallization of the device and substrate used for the die attach process [13].

This paper investigates the principal understanding of diffusion mechanism of Ag particles in Ag paste material at elevated temperature using Field Emission Scanning Electron Microscopy (FESEM) and Focused Ion Beam (FIB). This includes the examination of the Ag particles content, size, geometry and its distributions. The microstructure analysis on the surface and bulk properties of sintered Ag will lead to the understanding of the formation of bonding particles into a predominantly solid Ag network as a conducting path for the interconnect technology applications. The particle size, as well as the grain growth, will be studied in detail.

2. EXPERIMENTAL DETAILS

In this study, the Ag paste material consists of 80% metal content, 12% polymer material and 8% solvent. Figure 1 shows the as-received Ag paste sample in a syringe container. The Ag paste is dominated by spherical particles in sub-micron sizes.

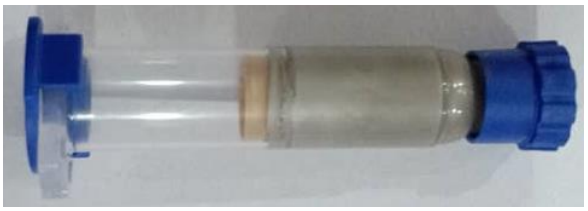

Figure 1. The as-received Ag paste sample.

The Energy Dispersive X-ray Spectroscopy (EDS) mapping analysis was conducted using FEI Transmission Electron Microscopy (TEM) Tecnai G2 F20 instrument to determine the composition of the Ag paste sample. TEM system uses Schottky Field Emission Gun to produce the primary electron beam and accelerated at 200 kV giving an imaging resolution of 0.2 nm. Figure 2 shows the sample preparation process before the EDS analysis. The process starts by transferring the Ag paste sample into 20 ml sample vial and mixed it with ethanol for dispersing

purpose. The sample was then sonicated for 20 minutes using an ultrasonic bath. A carbon coated copper grid was then used to mount the sample for EDS analysis.

(a) (b) (c)

Figure 2. (a) Ag paste dispersed in ethanol (b) Ultrasonic bath for a sonication process and (c) A carbon coated copper grid for mounting the Ag paste before EDS analysis.

The samples for microstructure evaluation were prepared by a manual printing technique. The as-received Ag paste was printed onto the silicon (Si) substrate with a dimension of 1.5 cm × 1.5 cm and left to dry under room temperature before the heat treatment process as shown in Figure 3. The sintering process was conducted in a high-temperature oven under normal atmospheric environment. The temperatures used in these experiments are 100°C, 200°C, 250°C, 275°C and 300°C for 2 hours storage. The sample that was dried in room temperature (RT) was used as a control sample in this study.

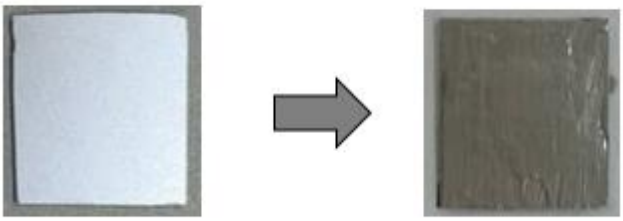

(a) **(b)**

Figure 3. (a) Si substrate and (b) Si substrate after printed with Ag paste.

The dual beam system of FEI Helios Nanolab 650 has a dual capability in performing Field Emission Scanning Electron Microscopy (FESEM) inspection as well as Focused Ion Beam (FIB) for micro-sectioning. The FESEM technique was employed to investigate the surface morphology as well as the surface interaction of the sintered Ag samples. The acceleration voltage of 5 kV and a beam current of 100 pA were set during the electron microscopy analysis. The imaging resolution of this instrument is 0.8 nm. Further FIB micro-sectioning analysis using the same system involves the use of gallium (Ga) ion that accelerated at 30 kV to precisely cut the samples for detailed examination at the cross-sectional view of the samples. Figure 4 shows the top view image of the FIB cut area. The analysed sample was deposited with platinum (Pt) before the FIB cutting process for protecting the sample surface from the bombardment of Ga ion as well as for minimizing the curtaining effect that could be induced by the sample surface. The FIB cutting process involves two steps namely rough cut and fine cut. The rough cut process utilizes high beam current approximately 21 nA to accelerate the removal of material. Upon completion of rough cut, the fine cut is performed at a lower beam current approximately 0.48 pA to produce a fine and high quality of finishing for further electron microscopy imaging at the sectioned area.

This technique allows the examination of the diffusion mechanism between the Ag particles as well as the investigation on the Ag particle and grain size growth to be carried out.

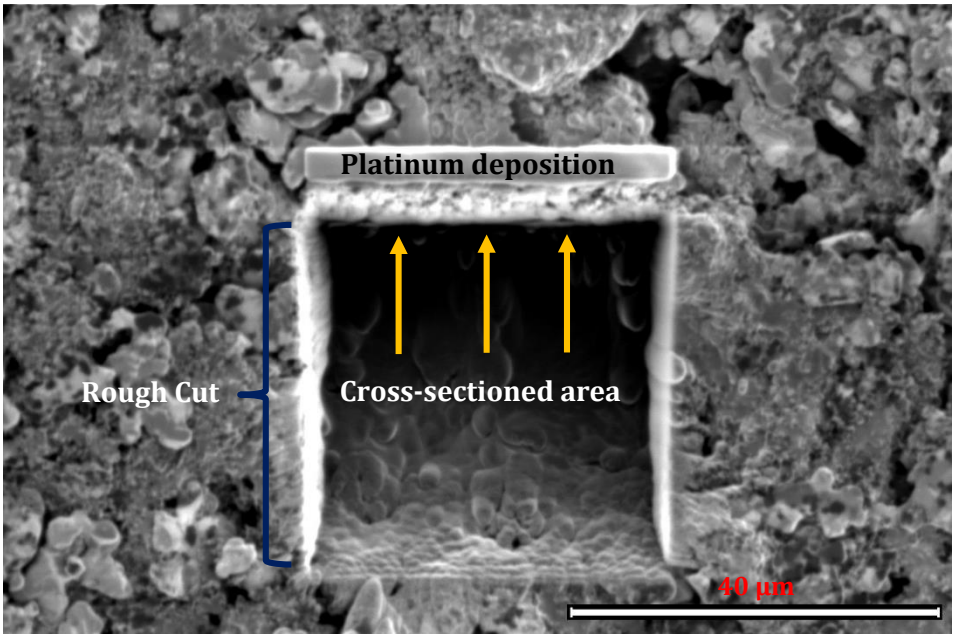

Figure 4. The FIB micro-sectioning technique.

3. RESULTS AND DISCUSSION

The as-received Ag paste material was analysed using electron microscopy before heat treatment process to investigate its initial filler geometry and distributions. Figure 5 (a) represents the electron micrograph of as-received Ag paste material that was acquired from the top view of the sample. It was observed that the Ag paste material consists of spherical Ag particles bounded by a polymeric material. The Ag particles are in submicron sizes with an average diameter of 420 nm. Figure 5 (b) shows the histogram distributions of Ag particles. The distributions of Ag particle size is relatively wide, this expectedly gives an advantage to the subsequence heat treatment process that the small particles may diffuse faster than bigger particles due to larger surface area [14]. Based on top view electron microscopy inspection, Ag particles were found to be loosely bounded and some are agglomerated within the polymer binder due to strong agglomeration effects between the particles. The agglomeration effects may also initiate rapid surface diffusion once thermal energy is being introduced during the heat treatment process. There was also an area with unoccupied Ag particles within the polymer binder, which appeared in dark contrast in electron micrograph image, and this will potentially result in voids formation as the polymer material evaporated during the sintering process.

Scanning Transmission Electron Microscopy (STEM) with an attachment of Energy Dispersive X-ray Spectrometry (EDS) systems was utilized to study the composition of Ag particles in the polymer binder on the as-received Ag paste sample before the heat treatment process. Figure 6 (a) indicates the STEM micrograph with elemental mapping region as marked in an orange box. It was observed that the Ag particles are dispersed and agglomerated within the polymer binder. Figure 6 (b), (c) and (d) represents the elemental mapping results of silver (Ag) in blue colour, carbon (C) in red colour and oxygen (O) in green colour respectively. The detection of C and O elements hypothetically is the evidence on the presence of polymer binder within the Ag paste material before the heat treatment process. It is expected that the polymer binder shall contain C, O and H (Hydrogen) elements, however, due to the limitation of EDS, the H detection is not

possible to be done and other characterization techniques such as FTIR might be necessary for hydrocarbon detection.

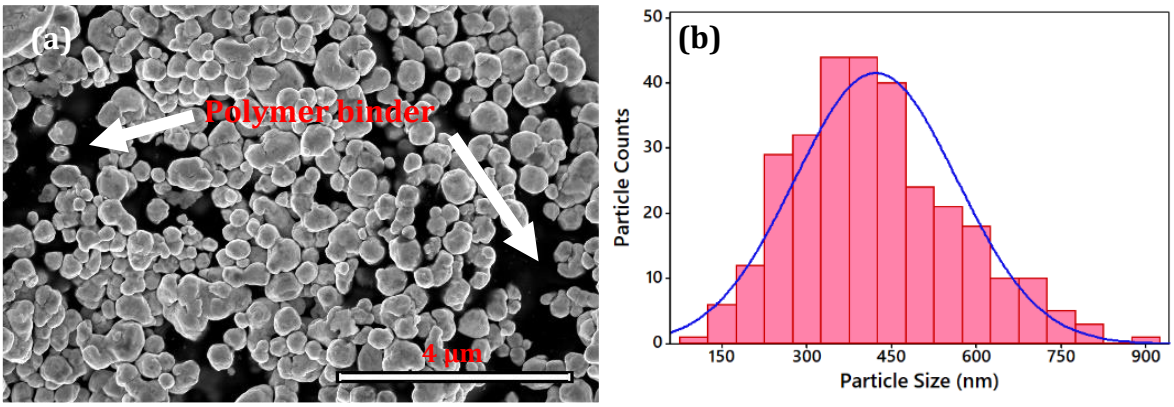

Figure 5. (a) The sub-micron spherical Ag particles and (b) size distributions.

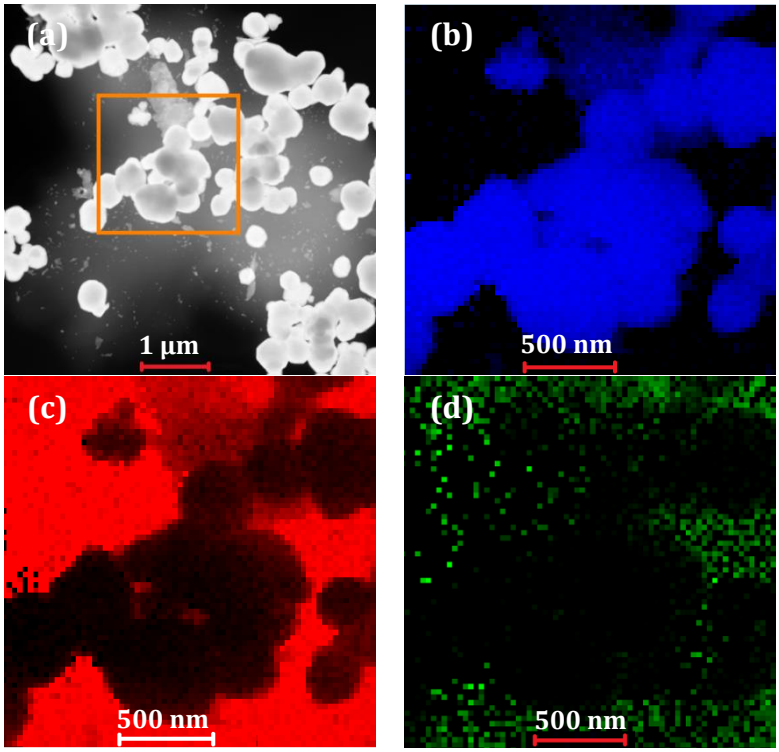

Figure 6. (a) STEM micrograph indicates the EDS elemental mapping region, (b) Ag mapping, (c) C mapping and (d) O mapping results.

3.1 Surface Diffusion

Figure 7 depicted the electron micrograph results that were acquired on the sample surface at RT and after heat treatment at the temperature of 100°C, 200°C, 250°C, 275°C and 300°C. Generally, heat treatment temperature plays an important role to enable the surface interaction between the Ag particles [15]. Sample at 100°C and 200°C were found to have similar surface morphology structure whereby negligible surface interaction can be observed between the Ag particles and its initial spherical shapes are maintained, which is similar with the Ag particle at RT. The evidence of surface interaction can be observed on the sample at 250°C, as more connecting particles exist. The particles bridge onto one and another but still maintaining its spherical shape. The joint and connection between the particles at this stage begun by the necking formation

between the particles. However, not all of the particles are making contact at the same time. It was clearly observed that the necking formation only occurred on relatively small particles. This is due to the surface interaction and connection is relatively low at 250°C that the thermal energy is sufficient to provide enough activation energy only on small particles to enable the connections. At heat treatment temperature of 275°C, it was observed that Ag particle has transformed from its original spherical shape to elongated structure and formed a bunch like networking between the Ag particles. As a result, a long chain of connecting particles was formed. At this stage, the necking between particles are much more visible and the size of the particles are further enlarged, as the thermal energy is sufficient to reduce the surface energy and to allow surface diffusion between the particles to take place [16]. The area that was preoccupied by the volatile polymer binder has progressively diminished at the temperature above than 275°C leading to the relatively solid formation of Ag network. This is due to the polymer binder that was used to bind the Ag particles has evaporated with the increasing of temperature and at the same time, the diffusion amongst the particles formed the diffusion network. At the temperature of 300°C, the width of the bunch like networking appeared to be narrower, as the Ag particles start to transform the shape into irregular structures.

The thermal energy attained from sintering process not only transformed the shape of Ag particle but also modifies the grain size of Ag particles. Figure 8 (a) to (f) are the magnified view of electron micrograph to allow detailed examination on the surface grain growth comparing the sample at RT and after the sintering process respectively. The grain boundary is less visible on the sample at RT. However, as the thermal energy is supplied to the sample, more defined and clear grain boundary could be observed on the sample. At 275°C and 300°C, the grain size appeared to be larger than the sample at a lower temperature. The mechanism of nucleation and growth of grain takes place once each grain starts to contact each other when temperature elevates [17]. The enlargement of grain size within the particle is associated with the grain boundary diffusions between Ag atoms since the supplied thermal energy is sufficient for the atoms to overcome the barrier for the diffusion to take place [18]. The grain boundary contained a high concentration of defects from their crystallographic misalignment, therefore the diffusive transfer along the grain boundaries occurs much faster than in their bulk. Higher thermal energy supply also promotes faster grain boundary diffusion as well as the growth in the grain size [19]. The average surface grain size is 117 nm, 140 nm, 166 nm, 226 nm and 253 nm for heat treatment at 100°C, 200°C, 250°C, 275°C and 300°C respectively. At 300°C, the surface grain size growth is about 33% larger than the initial grain size of Ag particles at RT (85 nm).

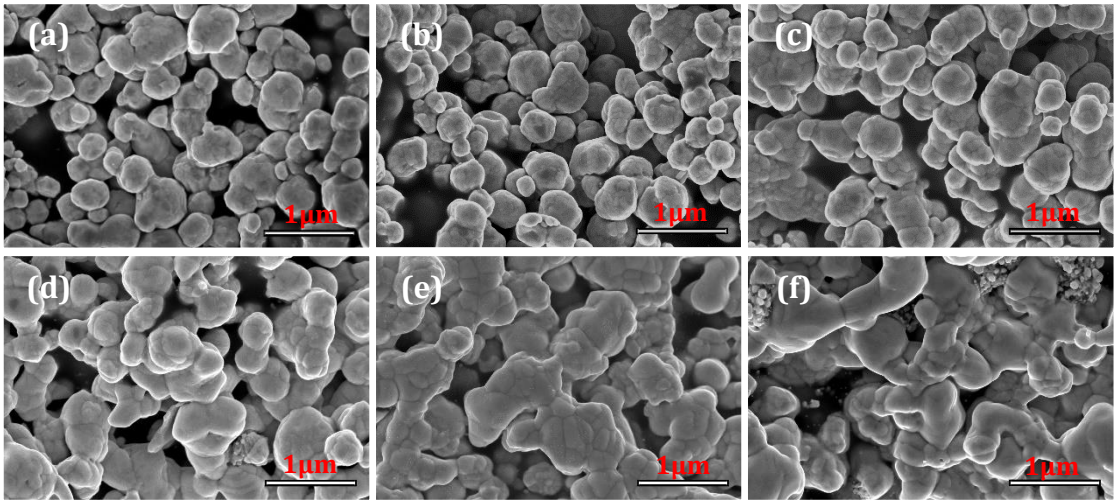

Figure 7. Surface interaction of Ag particles at (a) RT, (b) 100°C, (c) 200°C, (d) 250°C, (e) 275°C and (f) 300°C.

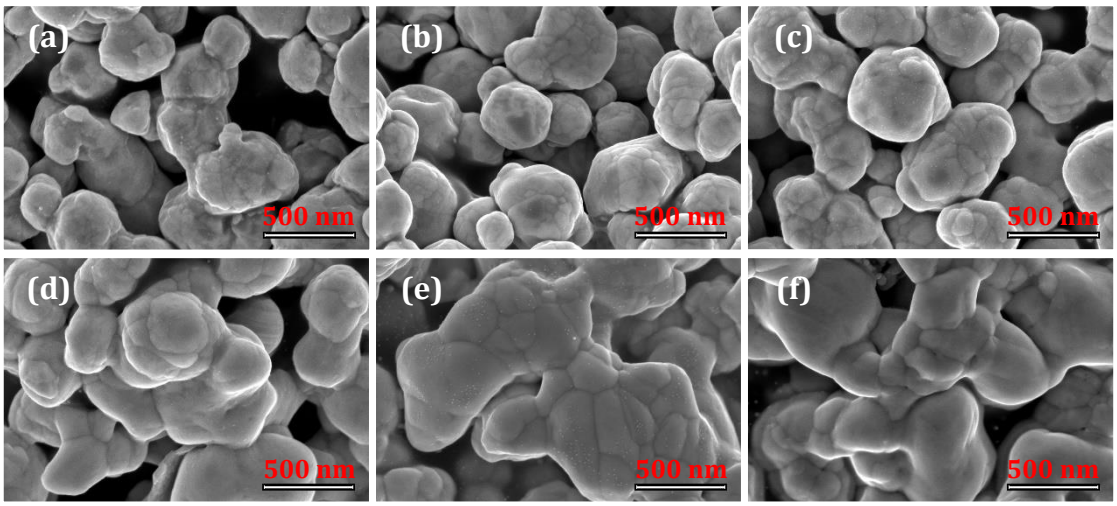

Figure 8. The comparison of surface grain growth between (a) Sample at RT, (b) 100°C, (c) 200°C, (d) 250°C, (e) 275°C and (f) 300°C.

3.2 Bulk Diffusion

In order to understand the bulk diffusion mechanism in the polymer binder, a FIB micro-sectioning analysis was conducted on the samples. Figure 9 represents the FIB cross-sectional view of the samples at RT and at an elevated temperature while Figure 10 is the magnified view of the sample at 250°C, 275°C and 300°C. At RT, it can be observed that some of the Ag particles are agglomerated and some already in contact even without the thermal energy, however, it can be seen that some of the Ag particles are scattered far from each other. It is also noted that the shape of Ag particles is nearly spherical with irregular edges due to the possible effect from the polymer binder itself. Additionally, based on the same field of view of the electron micrograph image, the particle counts at RT is lesser as compared with the sample that was subjected to the heat treatment process. Once the thermal energy is being introduced, the Ag particles start to make an intimate contact as can be seen at 100°C, 200°C and 250°C. More connecting particles can be seen at 250°C as compared to 100°C and 200°C. At this temperature range, the Ag particles show a slightly elongated shape with the enlargement of the particle size. At 275°C, a long chain of connecting particles can be observed with increasing of necking size as compared with the sample at 200°C and 250°C. The particle size enlargement is also more significant at 275°C and most of the connecting particle has transformed the shape into irregular structures. At 300°C, a complete formation of solid Ag material can be observed with the minor leftover of the polymer binder. In this study, the Ag particles are fully sintered at 300°C, that the sintering temperature has enabled the bonding between particles, which eventually forms solid structure via mass transport event that often initiate at the atomic level [20].

The driving force for the surface diffusion to take place is the reduction of surface energy on the particle surface [21]. This can be achieved by introducing the thermal energy to the Ag particles via heat treatment or sintering process. In this experiment, the activation energy to enable the sintering of Ag is as low as 250°C, that it enable the surface diffusion to take place which far below than the melting temperature of bulk Ag (961.8°C).

The presence of void formations can be seen as low as at 200°C. The void increase in size at 250°C and 275°C. Further higher temperature enlarges the void into a microporous growth. The microporous structure is getting visible at the sintering temperature of 300°C. According to the previous study, the porosity level and pore size in sintered Ag shown a significant effect to its thermal stability and fracture resistance [22-24].

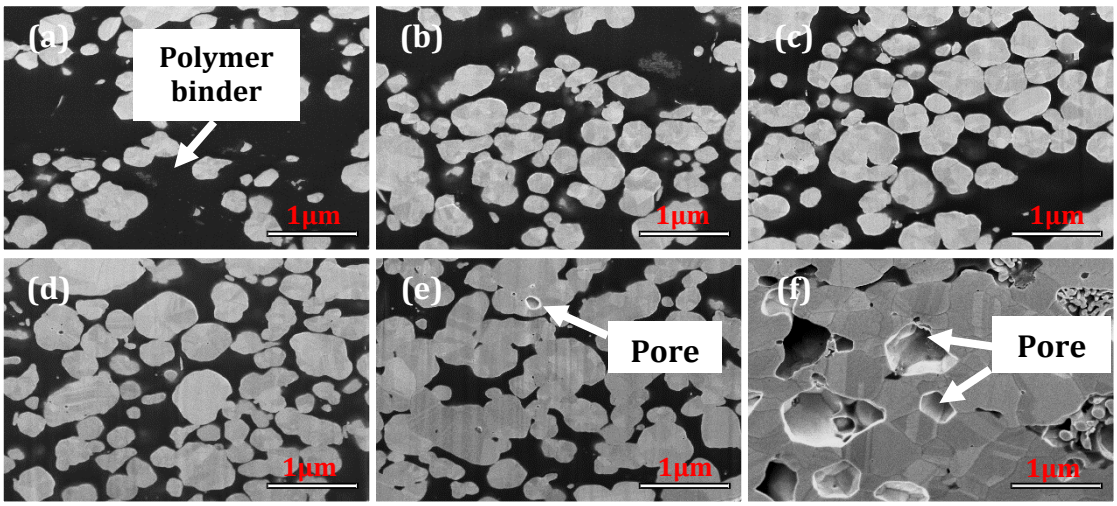

Figure 9. FIB cross sectional view of (a) RT, (b) 100°C, (c) 200°C, (d) 250°C, (e) 275°C and (f) 300°C.

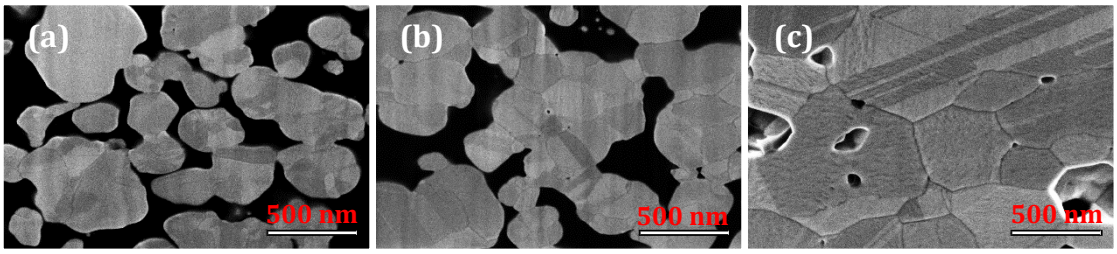

Figure 10. Magnified FIB cross sectional view of (a) 250°C, (b) 275°C and (c) 300°C.

Figure 11 illustrates the diffusion mechanism that results in the connection and bonding between Ag particles. Initially, two Ag particles come into intimate contact and the formation of necking structure appeared between the Ag particles as the atoms move from the surface of the two particles and diffused. Further atom movement and diffusion between the particles neck increase the neck size. The necking structure becomes broader and thicker as the temperature continuously elevated. Finally, further surface diffusion leads to the enlargement of particle size as well as the transformation of the particle shape from spherical to elongated structure. This phenomenon eventually results in the formation of a long chain of connecting particles, which transform the Ag particles into solid Ag network.

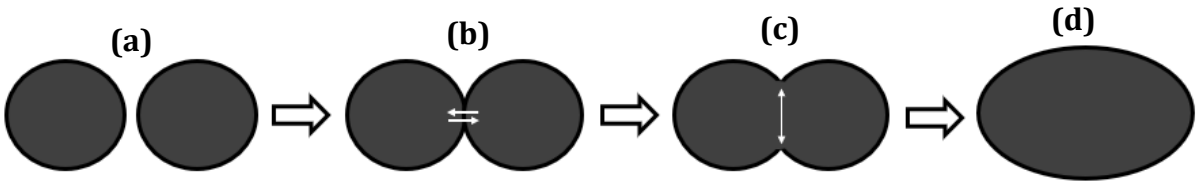

Figure 11. The diffusion mechanism of Ag particles (a) Ag particles initiates intimate contact, (b) initiation of surface diffusion, (c) necking growth, (d) particle growth and forming an elongated shape.

Figure 12 represents the plot of particle versus grain size of the sample at an elevated temperature that was measured based on FIB cross-sectional analysis as in Figure 9. It was observed from the graph that the grain size within the particle is increase with the increasing of the particle size. The rate of particle size growth is 3 to 4 times higher than the growth of the grain size. This is because the thermal energy during the heat treatment process that was supplied to the Ag filled epoxy system initially will cause surface diffusion. Once the surface diffusion

completed, the continuous supply of thermal energy to the system will cause the grain boundary diffusion within the particles resulting in the formation of the bigger grain size [25].

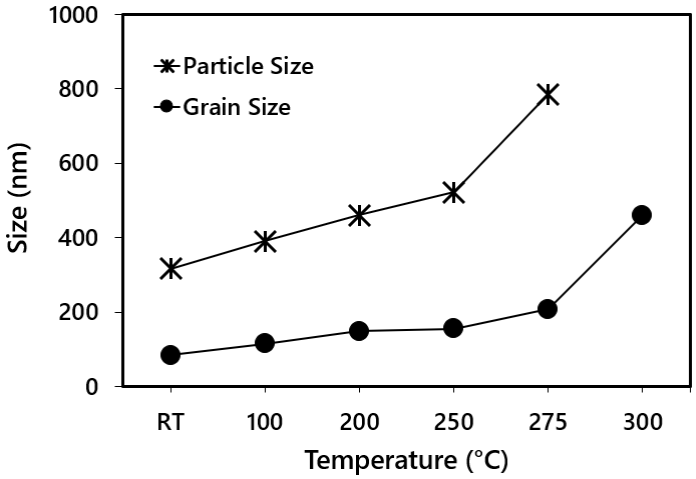

Figure 12. The graph of particle size and grain size at elevated temperature.

4. CONCLUSION

The electron microscopy technique revealed that the surface diffusion initiated between Ag particles as they come into intimate contact through the formation of necking. Further atomic movement and diffusion between the particles neck resulting in a volume contraction, necking growth as well as a transformation of the particle into a long chain of connecting particles. The small particles diffuse faster than the bigger particles due to its large surface area to volume ratio provides high activation energy for surface diffusion. The formation of grain growth among diffused particles was observed after the completion of surface diffusion. The solid state diffusion among the particles and its grain boundary diffusions resulted in the formation of micropores in the sintered Ag network.

ACKNOWLEDGEMENTS

The authors are gratefully acknowledged the Advanced Manufacturing Centre (AMC), Lab Research Advanced Materials Characterization Laboratory (AMCHAL), the financial support from Universiti Teknikal Malaysia Melaka, Ministry of Education, Malaysia under FRGS Grant, Project no. FRGS/2018/FKM/ F0366. The authors also would like to acknowledge Dr Shutesh Krishnan from ON Semiconductor (M) Sdn. Bhd. for his help in this publication.

REFERENCES

[1] Roccaforte, F., Fiorenza, P., Greco, G., Nigro, R. L., Giannazzo, F., Iucolano, F.,& Saggio, M, "Emerging trends in wide band gap semiconductors (SiC and GaN) technology for power devices" **187** (2018) 66–77.

[2] Shur, M., "Wide band gap semiconductor technology: State-of-the-art", Solid-State Electronics **155** (2019) 65–75.

[3] Nishimoto, S., Moeini, S. A., Ohashi, T., Nagatomo, Y. & McCluskey, P., "Novel silver die-attach technology on silver pre-sintered DBA substrates for high temperature applications", Microelectronics Reliability **87** (2018) 232–237.

[4] Huang, Y., Luo, Y., Xiao, F. & Liu, B., "Failure mechanism of die-attach solder joints in IGBT modules under pulse high-current power cycling", IEEE Journal of Emerging and Selected Topics in Power Electronics **7.1** (2018) 99–107.
[5] Manikam, V. R. & Cheong, K.Y., "Die attach materials for high temperature applications: A review", IEEE Transactions on Components, Packaging and Manufacturing Technology **1.4** (2011) 457–478.
[6] Kim, S., Kim, K. S., Kim, S. S. & Suganuma, K., "Interfacial reaction and die attach properties of Zn-Sn high-temperature solders", Journal of Electronic Materials **38.2** (2009) 266–272.
[7] Siow, K. S., "Are sintered silver joints ready for use as interconnect material in microelectronic packaging?", Journal of Electronic Materials **43.4** (2014) 947–961.
[8] Yoon, J. W., Back, J. H. & Jung, S. B., "Effect of surface finish metallization on mechanical strength of Ag sintered joint", Microelectronic Engineering **198** (2018) 15–21.
[9] Siow, K. S. & Lin, Y. T., "Identifying the development state of sintered silver (Ag) as a bonding material in the microelectronic packaging via a patent landscape study", Journal of Electronic Packaging **138.2** (2016).
[10] Sabbah, W., Azzopardi, S., Buttay, C., Meuret, R. & Woirgard, E., "Study of die attach technologies for high temperature power electronics: Silver sintering and gold–germanium alloy", Microelectronics Reliability, 53.9-11 (2013) 1617–1621.
[11] Zhang, H., Li, W., Gao, Y., Jiu, J. & Suganuma, K., "Enhancing low-temperature and pressureless sintering of micron silver paste based on an ether-type solvent", Journal of Electronic Materials **46.8** (2017) 5201–5208.
[12] Chen, C., Suganuma, K., Iwashige, T., Sugiura, K. & Tsuruta, K., "High-temperature reliability of sintered microporous Ag on electroplated Ag, Au, and sputtered Ag metallization substrates", Journal of Materials Science: Materials in Electronics **29.3** (2018) 1785–1797.
[13] Paknejad, S. A. & Mannan, S. H., "Review of silver nanoparticle based die attach materials for high power/temperature applications", Microelectronics Reliability, **70** (2017) 1–11.
[14] Sugiura, K., Iwashige, T., Tsuruta, K., Chen, C., Nagao, S., Sugahara, T. & Suganuma, K., "Thermal stability improvement of sintered Ag die-attach materials by addition of transition metal compound particles", Applied Physics Letters, 114.16 (2019) 161903.
[15] Suganuma, K., Sakamoto, S., Kagami, N., Wakuda, D., Kim, K. S. & Nogi, M., Low-temperature low-pressure die attach with hybrid silver particle paste. Microelectronics Reliability, 52.2 (2012) 375–380.
[16] Parker, G., "Encyclopedia of materials: science and technology", (2001) 3703–3707.
[17] Offerman, S. E., Van Dijk, N. H., Sietsma, J., Grigull, S., Lauridsen, E. M., Margulies, L., Poulsen, H. F., Rekveldt, M. T. & Van der Zwaag, S., "Grain nucleation and growth during phase transformations", Science, 298.5595 (2002) 1003–1005.
[18] Ahmad, I. F., Omar, G. & Salim, M. A., "Extrinsic Activation Energy for Enhanced Solid-State Metallic Diffusion for Electrical Conductive Ink", Journal of Advanced Research in Fluid Mechanics and Thermal Sciences **50** (2018) 32–39.
[19] Chen, C., Zhang, Z., Wang, Q., Zhang, B., Gao, Y., Sasamura, T., Ma, N. & Suganuma, K., "Robust bonding and thermal-stable Ag–Au joint on ENEPIG substrate by micron-scale sinter Ag joining in low temperature pressure-less", Journal of Alloys and Compounds, (2020) 154397.
[20] German, R. M., "Coarsening in sintering: grain shape distribution, grain size distribution, and grain growth kinetics in solid-pore systems", Critical reviews in solid state and materials sciences **35.4** (2010) 263–305.
[21] German, R. M., "Sintering trajectories: description on how density, surface area, and grain size change" Jom **68.3** (2016) 878–884.
[22] Gadaud, P., Caccuri, V., Bertheau, D., Carr, J. & Milhet, X., "Ageing sintered silver: relationship between tensile behavior, mechanical properties and the nanoporous structure evolution", Materials Science and Engineering: A, **669** (2016) 379–386.
[23] Choe, C., Noh, S., Chen, C., Kim, D. & Suganuma, K., "Influence of thermal exposure upon mechanical/electrical properties and microstructure of sintered micro-porous silver", Microelectronics Reliability **88** (2018) 695–700.

[24] Zhao, Z., Zou, G., Zhang, H., Ren, H., Liu, L. and Zhou, Y.N., "The mechanism of pore segregation in the sintered nano Ag for high temperature power electronics applications", Materials Letters, 228 (2018) pp. 168–171.
[25] Esa, S.R., Yahya, R., Hassan, A. and Omar, G., "Nano-scale copper oxidation on leadframe surface", Ionics, 23.2 (2017) pp. 319–329.